Preprint
UCRL-JC-146559

Initial Reaction Steps in the Condensed-Phase Decomposition of Propellants

C.F. Melius, M.C. Piqueras

This article was submitted to
29th International Symposium on Combustion, Sapporo, Japan,
July 21-26, 2002

December 11, 2001

U.S. Department of Energy

Lawrence
Livermore
National
Laboratory

DISCLAIMER

Initial Reaction Steps in the Condensed-Phase Decomposition of Propellants*

Carl F. Melius§
Lawrence Livermore National Laboratory
Livermore, California 94550-9234, USA

and

Mari Carmen Piqueras
Departament de Química Física
Universitat de Valencia
46100 Burjassot, Spain

Preference: Oral

Colloquium topic area:

Combustion of Solid Fuels – Solid Propellants

Word count: 5420 = 3250 words + 420 (eqn) + 350 (ref) + 1 table (400) + 5 figures (1000)

§To whom correspondence should be sent:

Carl F. Melius
Telephone: 925-422-3753
Fax: 925-422-2628
e-mail: melius1@llnl.gov

* This work was performed under the auspices of the U.S. Department of Energy by the University of California, Lawrence Livermore National Laboratory under Contract No. W-7405-Eng-48.

Initial Reaction Steps in the Condensed-Phase Decomposition of Propellants*

Carl F. Melius

Lawrence Livermore National Laboratory

Livermore, California 94550-9234, USA

and

Mari Carmen Piqueras

Departament de Química Física

Universitat de Valencia, 46100 Burjassot, Spain

Abstract

Understanding the reaction mechanisms for the decomposition of energetic materials in the condensed phase is critical to our development of detailed kinetic models of propellant combustion. To date, the reaction mechanisms in the condensed phase have been represented by global reactions. The detailed elementary reactions subsequent to the initial NO_2 bond scissioning are not known. Using quantum chemical calculations, we have investigated the possible early steps in the decomposition of energetic materials that can occur in the condensed phase. We have used methylnitrate, methylnitramine, and nitroethane as prototypes for O-NO_2, N-NO_2 and C-NO_2 nitro compounds. We find the energetic radicals formed from the initial NO_2

bond scissioning can be converted to unsaturated non-radical intermediates as an alternative to the unzipping of the energetic radical. We propose a new, prompt oxidation mechanism in which the trapped HONO can add back onto the energetic molecule. This produces oxidation products in the condensed phase that normally would not be produced until much later in the flame. We have shown that this prompt oxidation mechanism is a general feature of both nitramines and nitrate esters. The resulting HONO formed by the H-atom abstraction will be strongly influenced by the cage effect of the condensed phase. The applicability of this mechanism is demonstrated for decomposition of ethylnitrate, illustrating the importance of the cage effect in enabling this mechanism to occur at low temperatures.

---

* This work was performed under the auspices of the U.S. Department of Energy by the University of California, Lawrence Livermore National Laboratory under Contract No. W-7405-Eng-48.

Introduction

Our understanding of the chemical processes in the burning of propellants has made great strides in the past decade with the development of detailed chemical kinetics models [1-9]. The majority of the effort has been in the modeling of RDX and HMX nitramine propellants [2-8], though some efforts have also been made in the modeling of nitrate esters [1,9]. Most of these detailed kinetics mechanisms have been applied to the gas phase. Our understanding of the condensed phase chemistry is limited to overall (global) reactions that attempt to reproduce the net reactions occurring in the condensed phase [10-16]. Experimental results by Brill and coworkers [13-16] have been instrumental in estimating these condensed-phase reactions under combustion conditions, but the reactions are global in nature.

It is believed that the initial step in the decomposition of nitramines and nitrate esters is NO_2 bond scissioning [10,17,18]. However, the next steps in the process are not clear. Simple unzipping of the energetic molecule does not explain all the various chemical species that are observed coming off the surface. Furthermore, autocatalysis occurs which further complicates the processes. The net activation energy of the collective process is typically significantly less than the initial NO_2 bond dissociation energy.

We therefore believe that it is important to develop elementary reaction steps for the condensed phase. In particular, it is important to develop the initial steps that lead to the branching pathways, after which global reactions for the individual branches can be utilized. Even under conditions simulating burning propellants, complex reaction processes are occurring. Brill and

coworkers [13-16] have detected products having high oxidation states, such as amides for nitramines and carboxylic acids for nitrate esters.

One challenge has been to identify the early reaction pathways that lead to these high oxidation states.

In this paper, we concentrate on the concerted (non-radical) reaction steps that might occur in the lower-temperature condensed phase of energetic materials. We propose a new prompt oxidation mechanism for nitramine and nitrate ester energetic materials involving HONO addition. This prompt oxidation mechanism is based on quantum chemical calculations of transition state structures for nitro-containing molecules. In the next section, we describe our theoretical approach. We then present reaction pathways for O-, N-, and C-nitro species and identify the key prompt oxidation reaction step. To test this new mechanism, we then present results for the decomposition of ethylnitrate. Finally, we discuss the ramifications of this new reaction mechanism for nitramines.

Theoretical Approach

The recently developed Bond-Additivity-Corrected G2 method (BAC-G2) [20] was used to determine the thermochemical properties of the reactants, products, and transition state structures for the methylnitrate, methylnitramine, and nitroethane calculations. The thermochemical properties used to develop the ethlynitrate detailed chemical kinetics mechanism were derived using the Bond-Additivity-Corrected Møller-Plessett 4th order perturbation method (BAC-MP4)

method [21]. The Gaussian quantum chemistry package was used for the electronic structure calculations.

The BAC-G2 method uses a higher level of theory than BAC-MP4. In particular, it uses a larger basis set including diffuse functions allowing it to treat ionic species. This is important since the elimination/addition reactions can incorporate ionic character and/or biradical character, making the BAC-MP4 method suspect. For instance, the five-centered HONO elimination first has the NO_2^- ion leaving followed by the proton hopping.

In Table I we present the heats of reaction and activation energies for NO_2 bond scissioning, HONO elimination, and HONO addition for nitroethane, methylnitramine, and methylnitrate, representing the C-NO_2, N-NO_2, and O-NO_2 moieties, respectively. We present the BAC-G2 results along with other levels of theory [20] (BAC-MP4, BAC-hybrid, BAC-DFT, G2, and DFT(B3LYP/6-31G*) for comparison. All methods give fairly consistent results, except for the DFT method, which consistently underestimates the heats of reaction for the radical products, overestimates the heat of reaction for the non-radical products, and underestimates the activation energy for HONO addition. The activation energy for HONO elimination for methylnitrate at the BAC-MP4 level is significantly underestimated, due to a large spin contamination. We consider the BAC-G2 results to be the most accurate and against which the other methods can be judged.

Several papers have investigated the initial steps in the decomposition of the nitramines RDX and HMX [21-25]. Based on our BAC-G2 results, it appears that the DFT results underestimate

the bond dissociation energies (BDEs) and activation energies, consistent with the conclusions of Harris and Lammertsma[26]. Our calculated BAC-G2 BDE for dimethylnitramine is 206.5 kJ-mol^{-1} compared to 217.3 kJ-mol^{-1} for methylnitramine, consistent with our original estimates using the BAC-MP4 method [21], though the BAC-G2 results are somewhat larger. Our BAC-G2 calculated activation energy for HONO elimination for dimethylnitramine is 196.2 kJ-mol^{-1} compared to 203.6 kJ-mol^{-1} for methylnitramine. We would expect the values for RDX and HMX to be similar to those for dimethylnitramine, larger than earlier theoretical estimates[21-25], but consistent with experimental data of Oxley et al.[17].

Initial Steps in Energetic Material Decomposition

In this section we present results for the initial bond breaking and rearrangement reactions that can occur in energetic materials containing nitro groups. We compare nitrate esters, nitramines, and nitroalkanes, representing, respectively, the O-nitro, N-nitro, and C-nitro groups. As prototypes, we present results for methylnitrate (CH_3ONO_2), methylnitramine (CH_3NHNO_2), and nitroethane ($CH_3CH_2NO_2$). These species represent the chemical moiety R-X-NO_2, where R is CH_3 and X is O, NH, and CH_2, respectively. The reaction coordinate diagrams, calculated at the BAC-G2 level of theory, are shown for each of these compounds in Figs. 1-3, respectively. The calculated heats of formation at 298K ($\Delta H_{f(298)}$) at the BAC-G2 level are given for each of the chemical species, including transition state structures. The resulting heats of reaction and activation energies for some of the key reactions are given in Table 1.

The initial decomposition step is NO_2 bond scission,

$CH_3XNO_2 \leftrightarrow CH_3X + NO_2$. (1)

For the nitrate esters and nitramines, the activation energy for formation of HONO, via a five-centered elimination,

$CH_3XNO_2 \leftrightarrow CH_2{=}X + HONO$. (2)

is slightly lower than that of NO_2 bond scission. However, the HONO elimination represents a tight transition state, and cannot compete with that of simple bond scission [21,23,27]. For nitroalkanes, reaction (1) is significantly more endothermic than the activation energy for the five-centered HONO elimination reaction (2). Thus, for nitroalkanes, reaction (2) can dominate reaction (1) at the low temperatures of the condensed phase.

The fate of the resulting products depends on the conditions of the environment (e.g., flame, detonation, cook-off, aging). At high temperatures, the NO_2 will diffuse away. At low temperatures, however, the cage effect temporarily keeps these initial products together. The NO_2 radical will readily abstract the weak C-H atom,

$CH_3X + NO_2 \leftrightarrow CH_2{=}X + HONO$. (3)

The fate of the HONO, like that of the NO2, will be strongly dependent on the cage effect. Besides the reverse of reaction (2), the HONO addition to form a nitro compound, we have identified a new reaction pathway, the addition of HONO to form the nitrite,

$$CH_2{=}X + HONO \leftrightarrow CH_2(ONO)XH. \quad (4)$$

For nitrate esters and nitramines, this six-centered addition reaction has a very low activation barrier (see Table I). Thus, it has a chance to compete with the HONO escaping from the cage (see next section).

The resulting nitrite can undergo a four-centered HNO elimination to form

$$CH_2(ONO)XH \leftrightarrow HC(O)XH + HNO. \quad (5)$$

It is also possible for the nitrite intermediate to undergo NO bond scissioning to form

$$CH_2(ONO)XH \leftrightarrow CH_2(O)XH + NO. \quad (6)$$

The resulting $CH_2(O)XH$ radical can then undergo C-X bond scissioning, forming CH_2O and the XH radical. For nitramines, the nitrite can undergo a separate four-centered C-N bond scissioning elimination, forming a primary nitramine.

$$CH_2(ONO)XH \leftrightarrow CH_2O + HXNO. \quad (7)$$

For nitrate esters, reaction (7) is the same as reaction (4).

Besides the sixth-centered HONO addition reaction to form the nitrite, HONO can undergo a four-centered addition reaction to form a hydroxyl group and a nitroso group,

$$CH_2{=}X + HONO \leftrightarrow CH_2(OH)XNO. \qquad (8)$$

For the nitrate ester this reaction (the dashed curve in Fig. 1) forms the same product as the six-centered reaction [isotopic labeling would show a difference]. For the nitramines, this four-centered addition leads to a new, more stable tautomer of the nitramine, which can undergo a four-centered elimination reaction that scissions the C-N bond,

$$CH_2(OH)XNO \leftrightarrow CH_2O + XNOH. \qquad (9)$$

These four-centered addition reactions (8) have higher activation energies than the six-centered addition reactions (4), but are lower than the five-centered addition reactions (2) to form the nitro compounds.

We denote reaction (4) to form the nitrite as the prompt oxidation pathway. Reaction (4) differs from the reverse of reaction (2) in that the HONO molecule has flipped around. Thus, the nitro group and H atom have been "swapped" between the fuel end (carbon) and oxidizer end (oxygen) of the nitrate ester. We have converted the nitrate ester to a more oxidized form, which

is thermodynamically more stable. This pathway short-circuits the normal gas-phase oxidation of alkoxyl species being converted to CO2 via CO. This mechanism can explain the condensed phase product formation of HCOOH observed by Brill and coworkers [13,16] in decomposition of nitrate esters and the product formation of amides in nitramines [12,15,28].

In addition to reaction (3), the NO_2 species can recombine with the resulting radical,

$$CH_3X + NO_2 \leftrightarrow CH_3XONO \leftrightarrow CH_3XO + NO, \qquad (10)$$

which can eliminate the nitroso group. While reaction (10) is a minor pathway for nitrate esters and nitramines, due to its endothermicity, the presence of the peroxyl radical has been detected in the aging of nitrate ester propellants [29].

For nitroalkanes, the X moiety in R-X-NO_2 is the same as the R moiety, i.e., both represent methylene groups, CH_2. Thus, the prompt oxidation pathway does not apply. Flipping the HONO to oxidize the carbon, reaction (4), forms the same product as reaction (10). While the nitrate esters and nitramines formed two different nitrites each, one more stable (reaction (4)) and one less stable (reaction (10)), the ethylnitrite is an average, which is slightly higher in energy than the nitroethane. Consequently, unlike the situations for nitrate esters and nitramines, the sixth-centered HONO addition (reaction (4)) for nitroalkanes has a higher activation energy than the five-centered HONO addition (reaction (2)).

Decomposition of Ethylnitrate

To investigate the significance of the prompt oxidation decomposition mechanism, we have created a simple model of the decomposition of nitrate esters. [As can be seen from Fig. 1 and 2, the decomposition of nitrate esters are somewhat simpler than nitramines.] For the prototype chemical species, we used ethylnitrate. The decomposition model was run at two different initial temperature conditions, 60C and 200C, corresponding to accelerated aging and to cook-off conditions. The 60C simulation was treated at constant temperature and pressure, while the 200C simulation was treated at constant volume. The density was taken to be that of liquid-phase ethylnitrate. The chemical reaction mechanism included 81 species and 455 elementary reactions. We used the SENKIN/CHEMKIN program [30] for the integration of the mass and energy conservation equations.

We ran two mechanism scenarios, one involving the cage effect (trapping) and one that did not. The CHEMKIN program is not designed to handle condensed-phase reaction mechanisms such as the cage effect. We therefore mention the specific modifications we made to the overall reaction mechanism to model the cage effect. We introduced two new species representing the CH_3CH_2O–NO_2 complex and the CH_3CHO–HONO complex, corresponding to these adducts trapped in the same cage in which they were created. The "–" symbol denotes the adduct complex within the cage. The thermodynamic properties for these complexes were determined using the BAC-MP4 method [21].

The gas-phase NO2 bond-scissioning reaction was replaced by two steps,

$$CH_3CH_2ONO_2 \leftrightarrow CH_3CH_2O\text{–}NO_2 \leftrightarrow CH_3CH_2O + NO_2 \quad (11)$$

where the first step represents the bond scissioning reaction occurring within the cage and the second step represent the escape of the NO_2 from the cage. The five-centered HONO elimination reaction was also replaced by two steps,

$$CH_3CH_2ONO_2 \leftrightarrow CH_3CHO\text{–}HONO \leftrightarrow CH_3CHO + HONO \quad (12)$$

where the second step allows the HONO to escape the cage.

Within the cage, we included the abstraction reaction,

$$CH_3CH_2O\text{–}NO_2 \leftrightarrow CH_3CHO\text{–}HONO \quad (13)$$

Finally, we included the prompt oxidation reaction,

$$CH_3CHO\text{–}HONO \leftrightarrow CH_3CH(ONO)OH \quad (14)$$

In addition, the HONO conversion reaction,

$$HONO + HONO \leftrightarrow H_2O + NO + NO_2 \quad (15)$$

was slowed by adding on a diffusion barrier to the activation energy. The rest of the reactions were treated as normal gas-phase reactions. In reality, modifications of all the reaction rates due to solvation and other dielectric effects, diffusion, acid-base catalysis and other ionic reactions, etc. should be made. However, we believe that these simple modifications should be sufficient to test the impact of the cage effect and our prompt oxidation mechanism on the decomposition process.

The thermodynamic properties for these complexes were determined using the BAC-MP4 method. The binding energies of the complexes were 6.3 kJ-mol^{-1} and 34.4 kJ-mol^{-1} respectively, the latter due to hydrogen bonding. Entropy of the complexes were underestimated since the contribution of hindered rotors were included but not that of restricted rotors. The activation energies of the rate constants were modified to include the binding energies of the complexes. The activation energies allowing the caged complexes to escape were augmented by an effective barrier height for diffusion. For this test case, a diffusion barrier of 10 kcal-mol^{-1} (42 kJ-mol^{-1}) was used. This barrier height represents the lower end of the range for diffusion of gases in polymers.

In Fig. 4, we show the species concentration profiles as function of time, without and with the cage effect (reactions (11) – (15)) for an initial temperature of 60C. One clearly sees a difference in the product formation between the two mechanisms, with the cage effect clearly enhancing the prompt oxidation mechanism forming the carboxylic acid rather than the nitroso compound.

The reaction pathway diagrams for the initial steps in the decomposition including cage effects are shown in Fig. 5. As one can see from Fig. 5b, at the higher temperature, the cage effect did not play a significant role, with the complexes breaking up and escaping the cage. At the lower temperature (Fig. 5a), one sees the prompt oxidation mechanism coming into play, forming acetic acid. [Using a larger diffusion activation energy would increase the role of the prompt oxidation mechanism at the higher temperatures.]

Normal formation of CO_2 in combustion is via CO, i.e., fuel $\rightarrow$ formaldehye/aldehyde $\rightarrow$ CO $\rightarrow$ CO_2, while this prompt oxidation mechanism allows CO_2 formation via the formic acid/carboxylic acid intermediate. The formation of formic acid is consistent with the SMATCH/FTIR results of Chen and Brill [13], who observed the formation of CO_2 and formic acid in the decomposition of various nitrate esters. We believe that the prompt oxidation mechanism is required for the observed formation of the formic acid and CO_2, since the temperature and species concentration just above the surface do not provide the proper OH radical concentration for the conversion of CO to CO_2 using normal combustion models.

Discussion

The ability to identify the initial elementary steps in the decomposition of energetic materials has been challenging due to the complex behavior of the condensed phase. Based on quantum chemical calculations, the first elementary step for both nitramines and nitrate esters should be the NO_2 bond scissioning reaction,

$$RHXNO_2 \leftrightarrow RHX{-}NO_2 \leftrightarrow RHX + NO_2, \quad (16)$$

followed by the abstraction reaction,

$$RHX{-}NO_2 \leftrightarrow R{=}X{-}HONO,\ RHX + NO_2 \leftrightarrow R{=}X + HONO, \quad (17)$$

where X = O or NR', and reaction (17) can occur either trapped in the cage or in the free state after diffusion. We have identified a new oxidation step,

$$R{=}X{-}HONO \leftrightarrow R(ONO)XH, \quad (18)$$

which we have denoted the prompt oxidation reaction, since it oxidizes the R group during the initial decomposition process. While reaction (18) can also occur in the free state after diffusion, we find that in the free state, the reaction cannot compete with HONO recombination (reaction (15)).

The key to developing reaction mechanisms is to identify places where branching in the reaction pathways can occur. Reactions (16)-(18), along with reaction (15), are key reactions, since they determine the fate of the NO_2 and HONO. Reaction (16) is a key reaction, since the NO_2 can escape the cage to undergo other oxidizing or abstraction reactions. The escape of NO_2 at higher temperatures prevents reaction (17), causing the RHX radical to unzip. Similarly, reaction (17) is a key reaction since the HONO can either undergo the prompt oxidation pathway or can escape the cage to undergo other reactions. In particular, the HONO molecule can react with

other HONO molecules (reaction 15) to reform NO_2 radicals. Thus, controlling the location of the HONO during the initial stages of decomposition is very critical to the overall decomposition process. Reaction (18) is a key reaction, since it leads to the non-radical unzipping of the molecule.

For nitramines, the HNO elimination reaction (5) produces the amide. The enol form of the amide, -C(O)NH- ↔ -C(OH)N-, provides a hydroxyl group next to an adjacent nitramine group, leading to C-N bond scissioning via a six-centered transition state,

$$RCH_2N(NO_2)C(OH)=NR' \leftrightarrow RCH_2NHNO_2 + R'NCO \qquad (19)$$

The primary nitramine can further unzip [21], via its aci-form, via a six-centered transition state to form methylenenitramines.

$$RN(NO_2)CH_2NN(O)OH \leftrightarrow RNHNO_2 + CH_2NNO_2 \leftrightarrow \ldots \qquad (20)$$

The nitrite adduct formed in reaction (18) can also form a primary nitramine (reaction (7)), also leading to reaction (20). This rapid unzipping of nitramines containing multiple nitramine groups is consistent with the experimental observations of Oxley et al.[17] The methylenenitramines can then decompose to form CH_2O and N_2O [21].

Besides leading to CH_2O and N_2O, the prompt oxidation mechanism (reaction (18)) can also explain the observed formation of amides and isocynates. Sequential NO_2 elimination, H atom

abstraction, HONO addition, and HNO elimination would also provide a mechanism for oxy-s-triazine formed in the decomposition of RDX observed by Behrens and Bulusu [28].

The relative importance of reactions (16)-(18) with respect to the cage effect will depend not only on the environmental conditions, such as heating rate, but also on the material properties, such as phase diagrams, diffusivity, etc. While we find that the molecular energetics for the elementary reactions for nitramines are quite similar [21,27], consistent with the experimental observations of Oxley et al. [17], the collective behavior can be quite different. We propose that a major difference between Cl20 and RDX/HMX, is the ability of the NO_2 to diffuse more readily in Cl20, thereby reducing the cage effect and the importance of our prompt oxidation mechanism. This would explain the greater production of NO_2 observed in the decomposition of Cl20 [31]. The relative importance of the cage effects will also be influenced by changes in the material characteristics in nanoenergetic material formulations.

Conclusions

Using quantum chemical calculations, we have investigated the initial steps in the decomposition of energetic materials that can occur in the condensed phase. In the lower temperatures of the condensed phase (relative to flame temperatures), energetic radicals formed from the initial NO_2 bond scissioning can be converted to unsaturated non-radical intermediates before the energetic radical can unzip. The resulting HONO formed by the H-atom abstraction will be strongly influenced by the cage effect of the condensed phase. In this paper, we have proposed a new, prompt oxidation mechanism in which the trapped HONO can add back onto the energetic

molecule. This produces oxidation products in the condensed phase that normally would not be produced until much later in the flame. We have shown that this prompt oxidation mechanism is a general feature of both nitramines and nitrate esters. The applicability of this mechanism was demonstrated for ethlynitrate, illustrating the importance of the cage effect in enabling this mechanism to occur at low temperatures.

Much work is needed to further develop these principles into detailed chemical kinetic models. A large database of elementary reactions to draw upon does not exist for the condensed phase as it does for the gas phase. In addition to diffusion properties and trapping properties, dielectric effects (solvation effects) and acid-base catalytic effects (ionic reactions) must also be considered. Modifications to chemical kinetics codes such as CHEMKIN are needed to treat the cage effects along with microscopic diffusion. In the mean time, development of mixed detailed chemical kinetic – global reaction mechanism must proceed, making sure that the elementary and global reactions are compatible with each other. We believe that the caged-induced prompt oxidation mechanism proposed in this paper will play an important role in these future developments.

References

1 Hatch, R.L., Proc. Twenty-Third JANNAF Combustion Meeting, CPIA Publ. 457, p. 157 (1986).

2 Melius, C.F., Proc. Twenty-Fifth JANNAF Combustion Meeting, CPIA Publ. 458, p. 155 (1988).

3 Melius, C.F., in Chemistry and Physics of Energetic Materials (S.N. Bulusu, Ed.), The Netherlands, 1990, p. 51.

4 Yetter, R.A., Dryer, F.L., Allen, M.T., and Gatto, J.L., J. Propul. Power 11:683 (1995).

5 Liau, Y.C. and Yang, V., J. Propul. Power 11:729 (1995); Liau, Y.-C., Kim, E.S., and Yang, V., Combust. Flame 126:1680 (2001).

6 Davidson, J.E. and Beckstead, M.W., Proc. Comb. Inst. 26:1989 (1996); Davidson, J.E. and Beckstead, M.W., J. Propul. Power 13:375 (1997).

7 Prasad, K., Yetter, R.A., and Smooke, M.D., Combust. Flame 115:406 (1998); Prasad, K., Yetter, R.A., and Smooke, M.D., Combust. Sci. Technol. 124:35 (1997).

8 Ermolin, N.E., and Zarko, V.E., Fizika Goreniya I Vzryva 37(2):3 (2001); ibid., Fizika Goreniya I Vzryva 37(3):3 (2001)

9 Miller, M.S., Anderson, W.R., in Solid Propellant Chemistry, combustion, and Motor Intrior Ballistics, Vol. 185 (V. Yand, T. B. Brill, and W. Z. Ren, Eds.), Progress Astr. and Aero., AIAA, Restron, VA, p. 501 (2000).

10 Fifer, R.A., in Fundamentals of Solid Propellant Combustion (K.K. Kuo and M Summerfield Eds) AIAA, Inc., New York, p. 177 (1984).

11 Schroeder, M.A., Fifer, R.A., Miller, M.S., Pesce-Rodriguez, R.A., McNesby, C.J.S., Singh, G., Widder, J.M., Combust. Flame 126:1577 (2001).

12 Brill, T.B., Arisawa, H., Brush, P.J., Gongwer, P.E., and Williams, G.K., J. Phys. Chem 99:1384 (1995); Brill, T.B., J. Propul. Power 11:740 (1995).

13 Chen, J.K., and Brill, T.B., Combust. Flame 85:479 (1991).

14 Thynell, S.T., Gongwer, P.E., and Brill, T.B., J. Propul. Power 12:933 (1996).

15 Gongwer, P.E. and Brill, T.B., Combust. Flame 115:417 (1998).

16 Brill, T.B., and Gongwer, P.E., Propellants, Explos. And Pyrotech. 22:38 (1997).

17 Oxley, J.C., Kooh, A.B., Szekeres, R., and Zheng, W., J. Phys. Chem. 98:7004 (1994).

18 Hiskey, M.A., Brower, K.R., and Oxley, J.C., J. Phys. Chem. 95:3955 (1991).

19 Waring, C.E., and Krastins, G., J. Phys. Chem. 74:999 (1970).

20 Melius, C.F., and Allendorf, M.D., J. Phys. Chem. 104:2168 (2000).

21 Melius, C.F., in Chemistry and Physics of Energetic Materials (S.N. Bulusu, Ed.), The Netherlands, 1990, p. 21.

22 Johnson, M.A., and Truong, T.N., J. Phys. Chem. A 103:8840 (1999).

23 Zhang, S., and Truong, T.N., J. Phys. Chem. A 104:7304 (2000).

24 Zhang, S., and Truong, T.N., J. Phys. Chem. A 105:2427 (2001).

25 Chakraborty, D., Muller, R.P., Dasgupta, S., Goddard, W.A., J. Phys. Chem. A 104:2261 (2000); ibid., J. Phys. Chem. A 105:1302 (2001).

26 Harris, N.J., and Lammertsma, K., J. Am. Chem. Soc. 119:6583 (1997).

27 Melius, C.F., Proc. Twenty-Fourth JANNAF Combustion Meeting, CPIA Publ. 476, p. 359 (1987).

28 Behrens, R., and Bulusu, S., J. Phys. Chem. 96:8877 (1992); ibid., J. Phys. Chem. 96:8891 (1992).

29 Kimura, J., Propellants, Explos. And Pyrotech. 14:89(1989).

30 A. E. Lutz, R. J. Kee, and J. A. Miller, Sandia Report SAND87-8248 (1987).

31 Patil, D.G., and Brill, T.B., Combust. Flame 87:145 (1991); Patil, D.G., and Brill, T.B., Combust. Flame 92:456 (1993).

Table I. Heats of reaction ΔH_{rxn} and activation energies ΔE at 300K for HONO elimination and R-NO2 bond scission using various quantum chemical methods, BAC-G2, BAC-MP4, BAC-Hybrid, BAC-DFT, G2, and DFT. Energies in kJ-mol.$^{-1}$

Reaction	BAC-G2	BAC-MP4	BAC-Hyb	BAC-DFT	G2	DFT
Heat of reaction ΔH_{rxn}						
$C_2H_5NO_2 \leftrightarrow C_2H_5 + NO_2$	122.5	120.6	123.7	118.7	124.3	116.8
$C_2H_5NO_2 \leftrightarrow C_2H_4 + HONO$	83.4	75.4	94.0	83.0	86.3	104.0
$C_2H_5ONO \leftrightarrow C_2H_4 + HONO$	74.0	69.1	79.9	79.0	77.5	93.7
$C_2H_5 + NO_2 \leftrightarrow C_2H_4 + HONO$	-186.5	-178.9	-169.8	-179.3	-187.2	-131.3
$CH_3NHNO_2 \leftrightarrow CH_3NH + NO_2$	217.3	211.5	217.4	216.2	222.0	195.0
$CH_3NHNO_2 \leftrightarrow CH_2NH + HONO$	8.6	4.3	23.9	20.6	12.9	44.9
$CH_2(ONO)NH_2 \leftrightarrow CH_2NH + HONO$	61.4	54.0	68.4	62.7	73.6	72.5
$CH_3NH + NO_2 \leftrightarrow CH_2NH + HONO$	-208.7	-207.2	-193.6	-195.6	-209.1	-150.1
$CH_3ONO_2 \leftrightarrow CH_3O + NO_2$	184.2	166.8	190.6	175.5	187.1	156.3
$CH_3ONO_2 \leftrightarrow CH_2O + HONO$	-68.0	-79.2	-60.4	-58.3	-65.4	-31.1
$CH_2(ONO)OH \leftrightarrow CH_2O + HONO$	175.5	165.7	173.3	179.3	188.9	180.9
$CH_3O + NO_2 \leftrightarrow CH_2O + HONO$	-252.2	-246.1	-251.0	-233.8	-252.6	-187.4
Activation Energy ΔE						
$C_2H_5NO_2 \leftrightarrow C_2H_4 + HONO$	202.1	203.0	194.0	176.9	201.5	190.0
$C_2H_5ONO \leftrightarrow C_2H_4 + HONO$	231.6	245.1	220.5	214.5	230.9	224.4
$C_2H_4 + HONO \leftrightarrow C_2H_5NO_2$	118.7	127.6	100.0	93.9	115.1	86.0
$C_2H_4 + HONO \leftrightarrow C_2H_5ONO$	157.6	176.0	140.5	135.5	153.4	130.8
$CH_3NHNO_2 \leftrightarrow CH_2NH + HONO$	203.6	196.6	196.9	185.3	202.7	198.5
$CH_2(ONO)NH_2 \leftrightarrow CH_2NH + HONO$	114.6	121.7	107.9	132.5	113.0	99.0
$CH_2NH + HONO \leftrightarrow CH_3NHNO_2$	194.9	192.3	173.0	164.8	189.8	153.6
$CH_2NH + HONO \leftrightarrow CH_2(ONO)NH_2$	56.9	61.7	40.2	75.4	51.8	28.0
$CH_3ONO_2 \leftrightarrow CH_2O + HONO$	181.7	138.3	168.5	161.1	180.1	174.2
$CH_2OHONO \leftrightarrow CH_2O + HONO$	115.4	109.1	110.1	81.5	113.3	96.1
$CH_2O + HONO \leftrightarrow CH_3ONO_2$	249.7	217.5	228.9	219.4	245.5	205.3
$CH_2O + HONO \leftrightarrow CH_2OHONO$	63.9	52.7	60.3	29.3	62.0	41.9

Figure captions

Figure 1. Reaction diagram for methylnitrate. The energy for the four-centered HONO addition to form the nitrite is given by the dashed curve. BAC-G2 heats of formation (in kJ-mol^{-1}) are given for reactants, products, and transition state structures.

Figure 2. Reaction diagram for methylnitramine. BAC-G2 heats of formation (in kJ-mol^{-1}) are given for reactants, products, and transition state structures.

Figure 3. Reaction diagram for nitroethane. BAC-G2 heats of formation (in kJ-mol^{-1}) are given for reactants, products, and transition state structures.

Figure 4. Concentration vs. time profiles for the products of decomposition of ethylnitrate at 60C (a) without trapping by the cage effect and (b) with trapping by the cage effect. CH_3CHO–HONO represents the caged adduct formed by CH_3CHO and HONO.

Figure 5. Reaction flow diagrams for decomposition of ethylnitrate at (a) 60C and (b) 200C. M represents a unimolecular reaction.

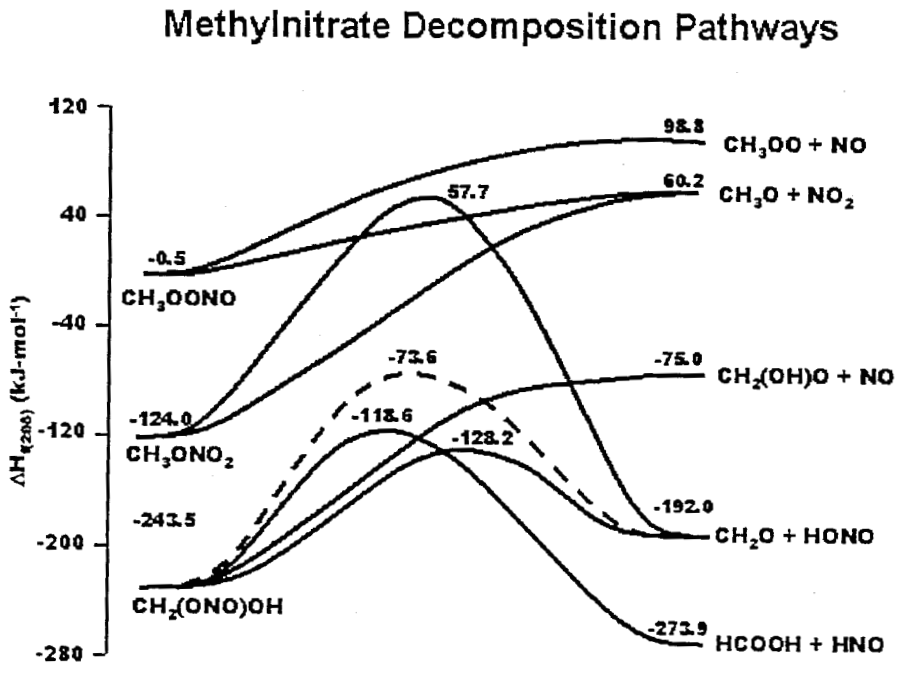

Figure 1. Reaction diagram for methylnitrate. The energy for the four-centered HONO addition to form the nitrite is given by the dashed curve. BAC-G2 heats of formation (in kJ-mol^{-1}) are given for reactants, products, and transition state structures.

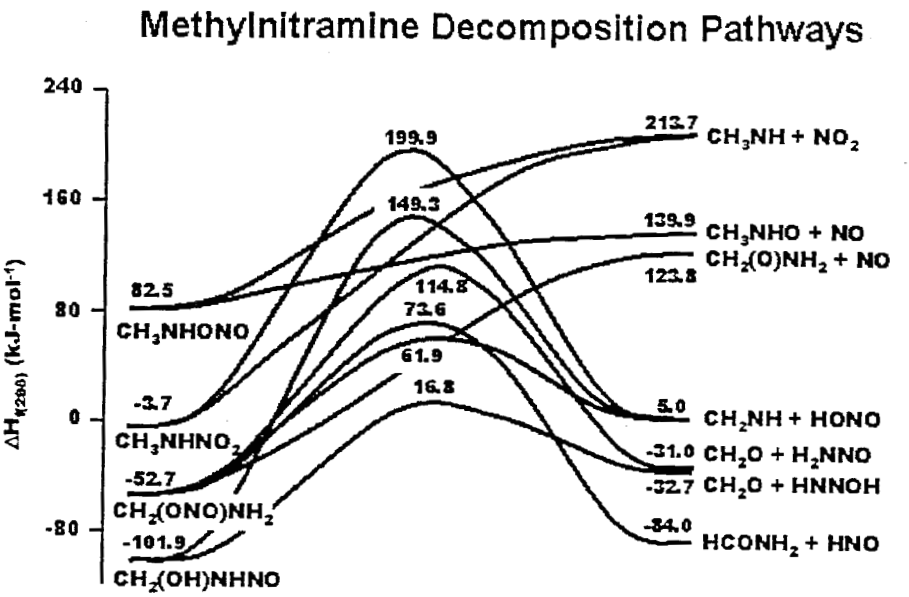

Figure 2. Reaction diagram for methylnitramine. BAC-G2 heats of formation (in kJ-mol^{-1}) are given for reactants, products, and transition state structures.

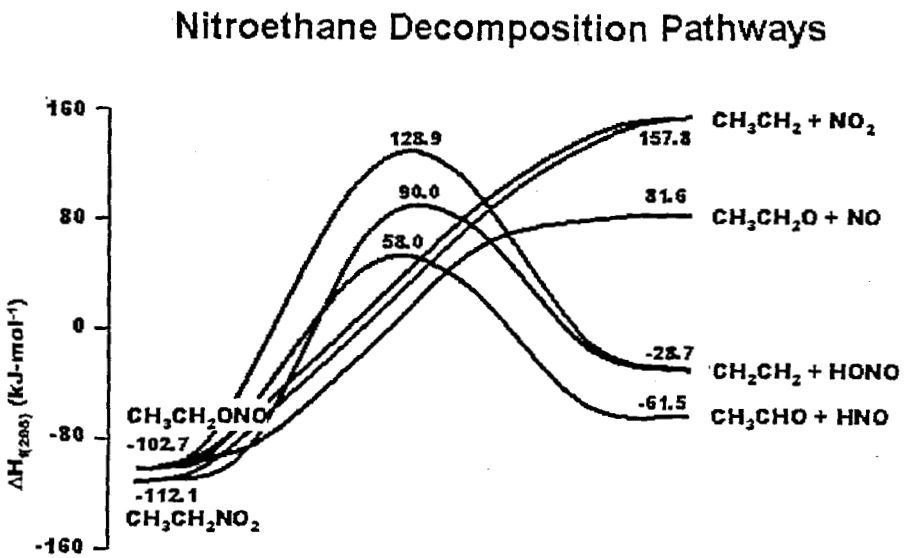

Figure 3. Reaction diagram for nitroethane. BAC-G2 heats of formation (in kJ-mol^{-1}) are given for reactants, products, and transition state structures.

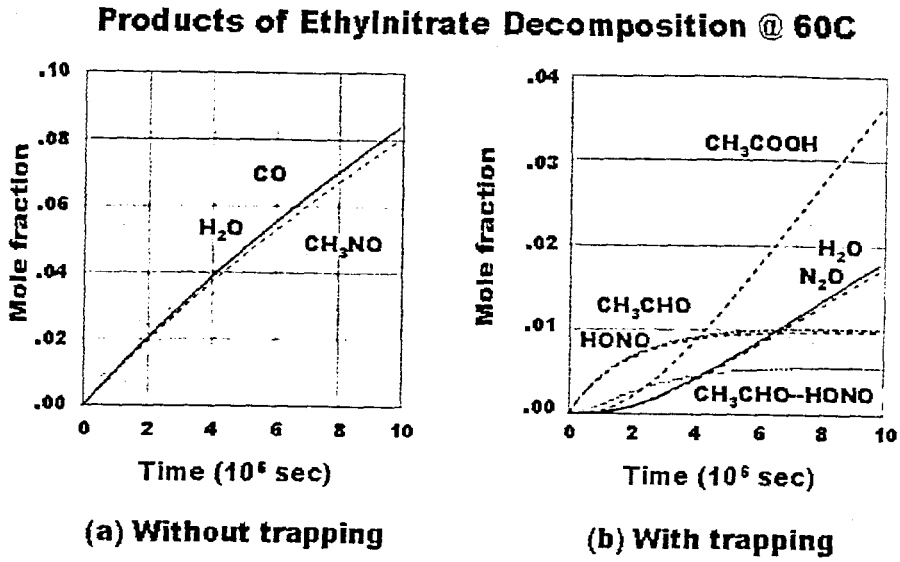

Figure 4. Concentration vs. time profiles for the products of decomposition of ethlynitrate at 60C (a) without trapping by the cage effect and (b) with trapping by the cage effect. CH_3CHO–HONO represents the caged adduct formed by CH_3CHO and HONO.

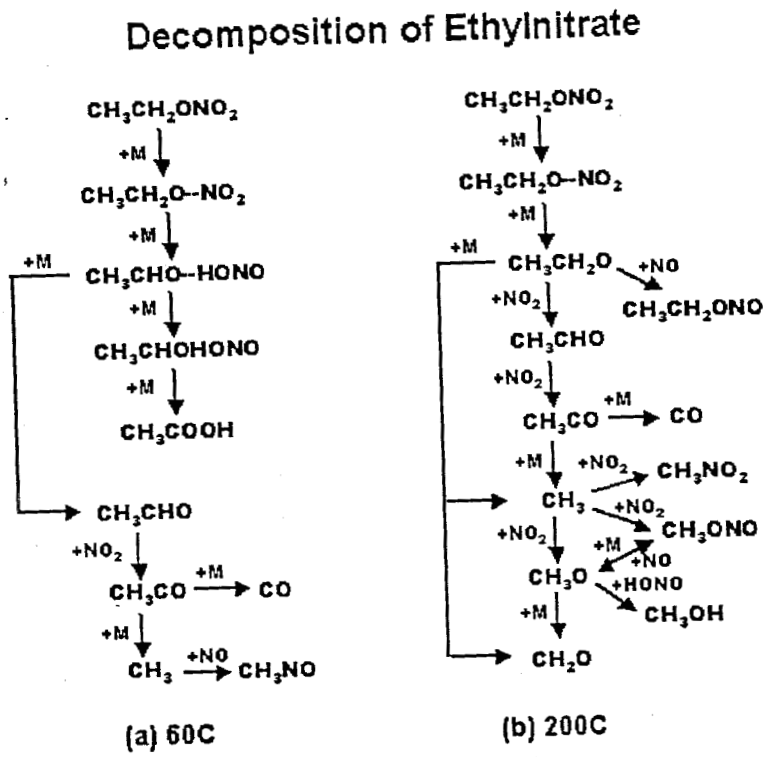

Figure 5. Reaction flow diagrams for decomposition of ethlynitrate at (a) 60C and (b) 200C. M represents a unimolecular reaction.